Remediation of a Railway Embankment on Collapsed Sensitive Glaciomarine Clay Using Timber Piles near Mink Creek, Northwest British Columbia

Adam Bontempo, Matthew Cormier, Chris Johnson, Kayla Robinson, & Tim Keegan
Klohn Crippen Berger, Vancouver, BC, Canada

Trevor Evans & David Brown
Canadian National Railway – Western Region

ABSTRACT
On the evening of November 25, 2020, an expansive earth flow landslide in a sensitive glaciomarine deposit destroyed approximately 130 m of track along the Canadian National Railway Company (CN) Kitimat Subdivision at Mile 9.42, approximately 10 km south of Terrace, BC. A site investigation and instrumented construction field trial program were conducted to assess the site conditions. Limit equilibrium and finite element methods were used to assess the stability of the embankment, and long-term settlement was estimated using both field and laboratory data. A combination of geosynthetics and timber shear piles were used to construct the new embankment, and additional instrumentation was installed to monitor changes in ground conditions during construction. This paper examines combinations of pile and geosynthetic elements and their capability to improve railway embankment stability in collapsed sensitive glaciomarine deposits.

RÉSUMÉ
Dans la soirée du 25 novembre 2020, un vaste glissement de terrain par écoulement de terre dans un dépôt glaciomarin sensible a détruit environ 130 m de voie le long de la subdivision Kitimat des Compagnie des Chemins de fer Nationaux du Canada (CN) au point milliaire 9,42, à environ 10 km au sud de Terrace, en Colombie-Britannique. Une enquête sur le site et un programme de remplissage d'essai instrumenté ont été menés pour évaluer les conditions du site. Des méthodes d'équilibre limite et d'éléments finis ont été utilisées pour évaluer la stabilité du remblai, et le tassement à long terme a été estimé à l'aide de données de terrain et de laboratoire. Une combinaison de géosynthétiques et de pieux de cisaillement en bois a été utilisée pour construire le nouveau remblai, et des instruments supplémentaires ont été installés pour surveiller les changements des conditions du sol pendant la construction. Cet article compare des combinaisons de pieux et d'éléments géosynthétiques et leur capacité à améliorer la stabilité des remblais ferroviaires dans les dépôts glaciomarins sensibles effondrés.

1 INTRODUCTION

On the evening of November 25, 2020, an earth flow landslide of approximately 300,000 m^3 destroyed approximately 130 m of track along the Canadian National Railway Company (CN) Kitimat Subdivision at Mile 9.42, approximately 10 km south of Terrace, BC. Due to the unique characteristics of the landslide, a background study, geotechnical investigation, and construction field trial program were conducted to better understand the site conditions and mechanism of failure. Upon completion, detailed design was carried out using the results of the investigation and field trial program. Due to the limited amount of time available to restore critical service to the track, a construction field trial program immediately followed the geotechnical investigation in order to quantify and observe several key input parameters required for geotechnical analyses.

2 BACKGROUND

A literature review was carried out to better understand the extensive history of landslides in the Mink Creek area. These landslides have been documented to be quite large in both volume and areal extent, with volumes exceeding 10 million m^3 and extending across areas of up to 2 km^2. These landslides have been observed to initiate at slope angles of less than 1˚ (Geertsema and Cruden 2008, Geertsema and Cruden 2014).

Within the past century, four significant landslides have been reported in the vicinity of Terrace, Prince Rupert, and Kitimat: the Mink Creek landslide in 1993, the Lakelse Lake road construction landslides in May and June of 1962, and a quick clay landslide on the Khyex River near Prince Rupert in 2003 (Geertsema and Schwab 1996). The Mink Creek landslide in 1993 occurred approximately 5 km south of Terrace and approximately 5 km north of the project area. The two Lakelse Lake landslides that occurred in 1962 were suspected to have a similar failure mode and

associated with, but not necessarily caused by, the nearby highway construction activities (Blais-Stevens 2017). Although there have been various studies carried out in the past to assess slope failures in glaciomarine clays, there is a lack of literature available pertaining to the reconstruction of linear infrastructure over failed glaciomarine clays.

3 GEOTECHNICAL INVESTIGATION

The geotechnical investigation consisted of cone penetration testing (CPT), field vane shear testing, advancement of mud rotary boreholes and test pits, as well as index and advanced laboratory testing. Drill holes and CPTs were completed to depths ranging from about 10 m to 60 m, both within and outside of the slide mass, to characterize the various material layers.

Due to the presence of slide debris and the very low shear strength of the surficial clay, creating access across the slide area was very challenging. Access roads and drill pads were constructed using logs that were available in the vicinity of the slide due to the significant number of fallen trees.

As part of the site investigation, eight vibrating wire piezometers and three slope inclinometers were installed within the slide mass to monitor movement and pore water pressures. This information was used to develop the baseline condition of the slide and monitor movement for potential further retrogression of the slide mass.

3.1 Subsurface Geotechnical Conditions

The major stratigraphic units identified are summarized in the following sections.

3.1.1 Organics

Organic soil and silty sand to sandy silt were encountered outside the landslide extents at the majority of the test hole locations from ground surface to depths of 0.1 m to 0.7 m.

3.1.2 Glaciomarine Clay Crust

Outside the landslide extents, the Glaciomarine Clay Crust was encountered either underlying the Organics or at ground surface to depths ranging from about 2 m to 4 m. This unit was generally classified as a firm to very stiff, brown, desiccated clay.

3.1.3 Earth Flow Colluvium

Within the landslide extents, the Earth Flow Colluvium was encountered from ground surface to depths of approximately 2 m to 4.5 m. This unit was generally classified as a very soft to firm, grey to brown clay.

3.1.4 Glaciomarine Clay

All test holes encountered the Glaciomarine Clay underlying either the Glaciomarine Clay Crust or Earth Flow Colluvium for a thickness of about 27 m to 55 m, terminating in the underlying Glacial Till. This unit was generally classified as a soft to firm, grey clay to silty clay, with variable amounts of sand closer to the bottom of the unit as it began to transition to the Glacial Till. The undrained shear strength of this unit was observed to increase approximately linearly with depth.

3.1.5 Glacial Till

The majority of the test holes terminated in the Glacial Till underlying the Glaciomarine Clay. The boreholes were advanced a maximum of about 7 m into the Glacial Till, and the CPT probe was unable to penetrate sufficiently far into the Glacial Till to obtain a significant amount of data. The Glacial Till primarily comprised silty sand and sandy silt.

4 CONSTRUCTION FIELD TRIAL PROGRAM

Instrumentation installed for the construction field trial program included vibrating wire piezometers, slope inclinometers, and settlement gauges. Test timber piles and H-piles were installed with re-strike testing, and dynamic pile load testing was carried out to assess the axial capacity of the piles. The construction field trial area consisted of multiple zones with various reinforcement combinations and was completed slowly over several days to optimize the final embankment design and the material placement rate.

During the preliminary design phase, potential remedial measures were discussed with CN, and the following three options were considered:

- Pile-supported embankment fill;
- Bridge; and
- Pile-supported embankment fill and partial bridge.

To explore those options a construction field trial program was carried out. The field trial program included constructing an embankment, installing geogrid, and driving both timber piles and H-piles. Pile Driving Analyzer (PDA) tests were carried out for the H-piles that were driven.

The pile-supported embankment fill option was chosen for the remedial measure based on the results of the field trial program and schedule constraints. In addition, several steel culverts would be installed at various locations and elevations along the embankment to divert surface runoff and potential future debris flows.

5 DESIGN

5.1 Timber Piles

5.1.1 Properties and Layout

Prior to construction, it was established that timber piles would be installed with a centre-to-centre spacing of about 1.0 m and that the piles would be an average of 15.2 m (50 ft) in length, with butt and tip diameters of approximately 360 mm (14 in) and 200 mm (8 in), respectively.

It was determined that the timber piles would be pushed or driven by an impact hammer through the Earth Flow Colluvium and into the Glaciomarine Clay as vibrating the piles would likely result in greater disturbance to the surrounding soils.

5.1.2 Allowable Shear Resistance

The allowable shear resistance of a rounded timber ($S_{allowable}$) can be calculated using the following equation, which is a rearrangement of the formula for calculating shear stresses in beams of circular cross-section (Gere and Goodno 2009):

$$S_{allowable} = 0.75 F_v A \quad [1]$$

Where:

F_v = Allowable shear stress perpendicular to the grain

A = Cross-sectional area of rounded timber

The average diameter of the timber piles was approximately 300 mm within the vicinity of the inferred slip surface. The allowable shear resistance of a 300 mm diameter timber pile was calculated to be about 58 kN assuming an F_v of 1,100 kPa for treated Douglas fir, as per Table 3-1 of the Timber Pile Design and Construction Manual (SPTA 2016). To account for the variability in pile diameter and the anticipated depth range of potential slip surfaces, an allowable shear resistance of 40 kN was used in the slope stability analyses.

5.2 Slope Stability Analysis

Limit equilibrium and finite element analyses were carried out to assess the stability of the proposed embankment slopes. The target live load Factor of Safety (FS) for downslope global embankment stability was 1.5. A major constraint on the analyses was that the embankment slopes had to remain within CN's right-of-way, which was particularly challenging for the upslope side.

The critical section modelled in all slope stability analyses was the highest section of the embankment. The section includes a 6.2 m high embankment, measured from the existing ground surface to the top of the ballast layer, with slopes of 2H:1V and 1.5H:1V on the downslope and upslope sides of the embankment, respectively.

5.2.1 Limit Equilibrium Analysis

Limit equilibrium was selected as the primary method for analyzing the slope stability of the proposed new embankment. The commercially available software program SLOPE/W (GEO-SLOPE 2020) was used to analyze the critical section.

5.2.1.1 Material Thicknesses and Properties

The major stratigraphic units presented in Section 3.1 were incorporated in the limit equilibrium model with the exception of the near-surface Organics unit, which was considered to have a negligible impact on slope stability due to its limited thickness and presence outside the slide area, a significant distance away from the new embankment. Thicknesses of natural materials were conservatively modelled such that the thicknesses of the weaker materials were closer to their upper bound / most representative values in the slide area (about 3.6 m to 4.5 m for the Earth Flow Colluvium and about 34.1 to 38.0 m for the Glaciomarine Clay), and the thickness of the stronger Glaciomarine Clay Crust was modelled as the lower bound value encountered (about 2.0 m). The ballast and sub-ballast were modelled with thicknesses of 0.5 m and 0.35 m, respectively.

Material properties were assigned based on a combination of in situ and laboratory testing results, literature review, and experience with similar materials. Table 1 summarizes the properties of the materials that were modelled using Mohr-Coulomb failure criterion.

Table 1. Mohr-Coulomb Material Properties Used in Limit Equilibrium Analysis

Material	Saturated Unit Weight (kN/m^3)	Effective Friction Angle (˚)	Effective Cohesion (kPa)
Ballast	20	45	0
Sub-ballast	20	40	0
Embankment Fill	19	38	0
Earth Flow Colluvium (Drained)	15	20	0
Glaciomarine Clay (Drained)	16	29	9

Table 2 summarizes the undrained properties of the cohesive materials that were modelled.

Table 2. Undrained Material Properties Used in Limit Equilibrium Analysis

Material	Saturated Unit Weight (kN/m^3)	Undrained Shear Strength (kPa)	Increase in Undrained Shear Strength with Depth (kPa/m)
Glaciomarine Clay Crust	18	46	-
Earth Flow Colluvium	15	7	-
Glaciomarine Clay	16	13 – 40	0.9
Glacial Till	20	200	-

5.2.1.2 Groundwater

For both the limit equilibrium and finite element analyses, groundwater was modelled using a single piezometric line across the section. The groundwater level was set at the ground surface across the slide area for all slope stability and settlement analyses carried out because most of the

test holes encountered groundwater at the surface. The piezometric line was modelled at depths up to about 1.7 m upslope of the head scarp and 6.5 m downslope of the toe of the slide, based on elevations that groundwater was encountered outside the slide extents.

5.2.1.3 Reinforcement Properties

Geosynthetics

Geosynthetic properties impacted only the local embankment stability as the global stability cases considered slip surfaces outside the geosynthetic reinforced zone of the embankment. As such, the properties discussed herein correspond to the local stability cases only.
Three layers of geogrid spaced at 0.3 m were included in total; the bottom layer consisted of geosynthetic biaxial geogrid and was modelled approximately 1.0 m above the existing ground surface (at the top of the timber piles), and the upper two layers consisted of uniaxial geogrid. The geocomposite biaxial geogrid and uniaxial geogrid were modelled with ultimate tensile strengths of 30 kN/m and 400 kN/m, respectively.

Reduction factors of 2.5 and 1.66 were applied to the ultimate tensile strengths for the geocomposite biaxial geogrid and uniaxial geogrid, respectively, resulting in factored tensile strengths of 12 kN/m and approximately 241 kN/m, in that order.

In calculating pullout resistance, an interface shear angle of 28˚ was input based on a formula presented in FHWA (2012) that relates the interface shear angle to the friction angle of the reinforced fill material.

Timber Piles

Timber pile reinforcements were manually drawn in the model with 15 m length and a 1.0 m centre-to-centre spacing. The out-of-plane spacing was set to 1.0 m to incorporate three-dimensional (3D) effects.

An allowable shear resistance of 40 kN was used in the analysis, as discussed in Section 5.1.2.

5.2.1.4 Modelling Methods

The Morgenstern-Price analysis method was used for all analyses as it considers both force and moment equilibrium and is considered to be the industry standard for the region.

The grid and radius option with radius tangent lines concentrated within the pile zone was used to calculate circular slip surfaces for the embankment stability analyses. The entry and exit option with radius tangent lines within the pile zone was selected to analyze the overall stability of the landslide.

A live load of 90 kPa was considered appropriate for modelling the vertical surcharge load induced by trains in the Kitimat Subdivision. The live load was modelled along a 2.6 m wide strip (equivalent to the length of a railway tie), centred on the top of the ballast.

5.2.1.5 Results

Several cases were analyzed for the critical section. Results are summarized in Table 3.

Table 3. Limit Equilibrium Slope Stability Results

Stability Case	Live Load FS
Downslope Global Embankment Stability	1.5
Downslope Local Embankment Stability	2.8
Downslope Global Embankment Stability with Upslope Surcharge Load	1.3
Upslope Local Embankment Stability	1.5
Downslope Global Embankment Stability Under Drained Conditions (Long-term Stability)	5.0
Overall Slope Stability	1.6

Global stability was assessed for the primary design case, where the minimum live load FS of 1.5 was achieved.

A live load FS of 2.8 was calculated for local embankment stability, which involved failure through the geogrid-reinforced zone of the embankment.

Global stability in the event of a retrogressive landslide was also analyzed, for which a FS of 1.3 was calculated and considered to be acceptable. In this case, material at the head scarp of the existing landslide would be dislodged and deposited on the upslope side of the embankment. The dislodged material was modelled such that it reached the top of the sub-ballast and that its unit weight would be equivalent to that of the Earth Flow Colluvium.

Embankment stability in the upslope direction was also analyzed, whereby a localized failure (i.e., through the geogrid-reinforced zone of the embankment) could occur. The live load FS for this case was 1.5.

The long-term live load FS was estimated to be significantly higher than the short-term; a FS of 5.0 was calculated using drained strength parameters for the Earth Flow Colluvium and Glaciomarine Clay.

Finally, the stability of the entire slope where the landslide occurred was analyzed by horizontally extending the search for slip surfaces. A FS of 1.6 was obtained for the critical slip surface, which extended from the Glaciomarine Clay Crust (approximately 110 m upslope of the head scarp), through the timber piles, and terminating about 20 m downslope of the embankment downslope toe.

5.2.2 Finite Element Analysis

Finite element was selected as a secondary method for analyzing the slope stability of the proposed new

embankment. The commercially available software program RS2 (Rocscience 2011) was used to analyze the critical section that was described in Section 5.2. This analysis was mainly carried out to compare the slip surfaces and associated FS with those obtained for various scenarios analyzed using the limit equilibrium method. Deformation of the critical section in response to gravitational and loading effects were also assessed for visualization purposes.

5.2.2.1 Material Thicknesses and Properties

Material thicknesses used in the finite element model were identical to those used in the limit equilibrium model. Since undrained material models cannot be used in a finite element analysis, all materials were modelled using Mohr-Coulomb failure criterion as this was the most applicable option. Tensile strength and effective residual cohesion were not assigned to any of the materials.

Strength properties of the materials modelled are summarized in Table 4.

Table 4. Material Strength Properties Used in Finite Element Analysis

Material	Saturated Unit Weight (kN/m^3)	Effective Peak Friction Angle (˚)	Effective Peak Cohesion (kPa)	Effective Residual Friction Angle (˚)
Ballast	20	45	0	0
Sub-ballast	20	40	0	0
Embankment Fill	19	38	0	0
Glaciomarine Clay Crust	18	27	0	0
Earth Flow Colluvium	15	20	0	6
Glaciomarine Clay	16	29	9	10
Glacial Till	20	35	0	0

Stiffness properties of the materials modelled are summarized in Table 5.

Table 5. Material Stiffness Properties Used in Finite Element Analysis

Material	Effective Elastic Modulus (MPa)	Effective Poisson's Ratio
Ballast	127	0.2
Sub-ballast	196	0.3
Embankment Fill	78	0.3
Glaciomarine Clay Crust	56	0.2
Earth Flow Colluvium	14	0.4
Glaciomarine Clay	16	0.4
Glacial Till	100	0.2

5.2.2.2 Reinforcement Properties

Geosynthetics

Three layers of biaxial geogrid spaced at 0.3 m were modelled. The bottom layer was modelled approximately 1.0 m above the existing ground surface, at the top of the timber piles. Each geogrid segment was modelled as a Geosynthetic Liner in RS2, with a tensile modulus of 800 kN/m, peak tensile strength of 18 kN/m, and residual tensile strength of 0 kN/m. The geocomposite biaxial geogrid had an ultimate tensile strength of 40 kN/m; a reduction factor of 2.25 was applied to this value for long-term strength loss as per FHWA (2012).

It was assumed that the geogrid would have no residual tensile strength, such that the geogrid would fail in a brittle manner.

Timber Piles

Timber pile reinforcements were manually drawn in the model with 15 m length and a 1.0 m centre-to-centre spacing. Each timber pile was modelled as a Standard Beam Liner in RS2, as recommended by Rocscience.

Since out-of-plane pile spacing could not be specified in the program, the timber piles were modelled with a continuous thickness of 0.3 m, such that they were represented as walls with a rectangular section in the out-of-plane direction. A sensitivity analysis showed that scaling down the strength and stiffness by a factor equivalent to the actual space that the piles would occupy in the out-of-plane direction made a marginal difference in the results.

Slip along the edges of the piles was not considered.

An Elastic Modulus of 10,000 MPa was input based on values presented in FPL (2010) and SPTA (2016).

A Poisson's Ratio of 0.3 was input based on values presented in FPL (2010).

A peak compressive strength of 8.6 MPa was input based on a value presented in SPTA (2016), which was more conservative than the values presented in FPL (2010). The timber piles were not considered to have any residual compressive strength.

A peak tensile strength of 2 MPa was input based on values presented in FPL (2010). The timber piles were not considered to have any residual tensile strength.

A unit weight of 4.4 kN/m^3 was input based on values presented in FPL (2010).

5.2.2.3 Modelling Methods

Plane strain analysis with Gaussian Elimination and effective stress analysis were selected for the finite element analysis. The strength reduction method was used to estimate the FS.

A gravity field stress type was used such that the in-situ stress field varies with depth. Two separate methods were used to calculate an effective stress ratio of 1.1 (rounded to 1 to account for uncertainty) near the contact between the Earth Flow Colluvium and Glaciomarine Clay; thus, this was an appropriate value to use in the analysis.

The ground surface was permitted to move freely in any direction while the right and left boundaries were constrained horizontally, the lower boundary was constrained vertically, and the bottom left and right corners were fixed.

Live loading was identical to that of the limit equilibrium analysis.

5.2.2.4 Results

Several stability cases were analyzed to calibrate and test the sensitivity of the finite element model, including total stress analysis vs. effective stress analysis, timber pile strength and stiffness properties, and mesh density. Results for the two main cases are summarized in Table 6 for the critical section.

Table 6. Finite Element Slope Stability Results

Stability Case	Live Load FS
Downslope Global Embankment Stability	1.8
Downslope Global Embankment Stability with Upslope Surcharge Load	1.5

5.2.3 Comparison of Slope Stability Analysis Methods

The live load FS values compared well for both methods. Though shallower slope failures were predicted using the finite element compared to limit equilibrium, the results of both methods were considered to be valid since both methods required their own unique set of assumptions, and both relatively shallow failures within the Earth Flow Colluvium and slightly deeper failures within the pile zone of the Glaciomarine Clay are considered feasible. Overall, the final embankment design met the minimum live load FS requirement of 1.5 for slope stability.

5.3 Settlement Analysis

Settlement analyses were carried out using the commercially available software Settle3 (Rocscience 2020) to assess the railway track's long-term anticipated total settlement and maximum differential settlement between the rails.

5.3.1 Material Thicknesses and Properties

The Earth Flow Colluvium and Glaciomarine Clay were modelled with thicknesses of 3 m to 4.5 m and 27 m to 34 m, respectively, within the timber pile embankment area. The thickness of the Glacial Till was unknown because the test holes that encountered this layer terminated within it. This layer was assumed to extend to a depth of 80 m in the Settle3 model, which was below the zone of stress influence from the embankment.

Material properties were estimated using available field and laboratory data collected during the geotechnical investigation and the field trial program and are presented in Table 7.

Table 7. Material Properties Used in Settlement Analysis

Material	Earth Flow Colluvium	Glaciomarine Clay	Glacial Till
Saturated Unit Weight (kN/m^3)	15	16	20
Poisson's Ratio	0.4	0.4	0.2
Constrained Modulus for Initial Loading (MPa)	14	16	100
Constrained Modulus for Reloading (MPa)	14	16	100
Primary Compression Index	0.53	0.46	-
Recompression Index	0.15	0.06	-
Initial Void Ratio	1.15	1.1	-
Overconsolidation Ratio	1	2	-
Coefficient of Consolidation (m^2/yr)	18	6.5	-
Recompression Coefficient of Consolidation (m^2/yr)	18	6.5	-
Secondary Compression Index	0.004	0.004	-
Secondary Recompression Index	0.004	0.004	-

5.3.2 Modelling Methods

The 3D vertical stress distribution in the soil stratum was calculated using the Multiple-Layer Stress Computation Method, which accounts for the effect of material layer stiffness on stress distribution.

A horizontal native ground surface was modelled. Embankment Loads by Layer were used to model the new fill areas. Embankment fill above the existing ground surface was modelled using an equivalent unit weight of 19 kN/m^3. Settlement of the embankment fill material and transient live loads were not analyzed as these were considered to have a negligible impact on the analysis.

Models were developed at 15 m intervals to account for the variation in embankment height along the alignment. An attempt was made to model the timber piles; however, this was not feasible as the stiffness contrast between the piles and the surrounding soil was greater than the program could account for. The results of settlement monitoring during the construction field trial indicated that total settlement was approximately 70% lower in the area where

timber piles were installed at a spacing of 1.0 m compared to where no piles were installed. These results were applied to the total settlement along the track alignment by multiplying the calculated settlement within the timber pile region by a factor of 0.3 and adding this value to the calculated settlement below the timber piles.

5.3.3 Results

Figure 1 presents the anticipated total settlement at the critical section for time periods ranging from one month to 25 years post-construction.

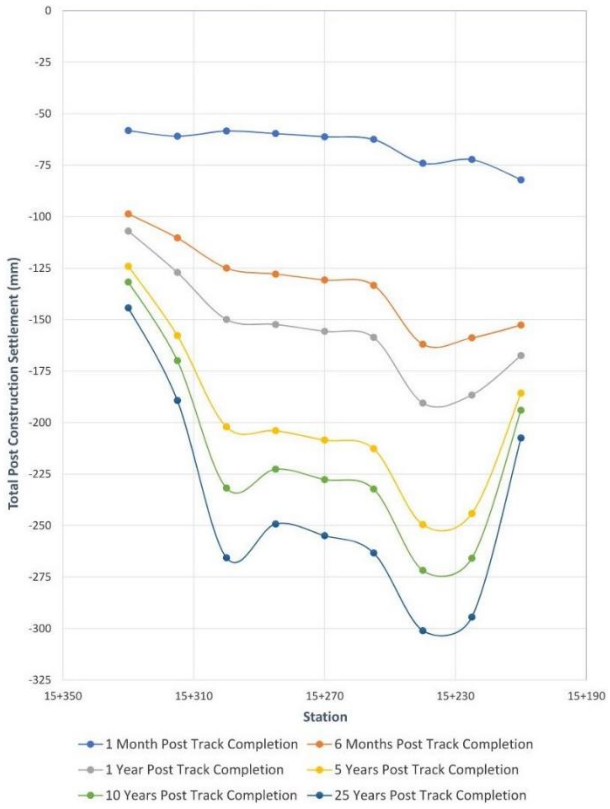

Figure 1. Anticipated Total Post-Construction Settlement

Figure 2 presents the anticipated maximum differential settlement profile at the section with the most variable ground surface, for time periods ranging from one month to 25 years post-construction.

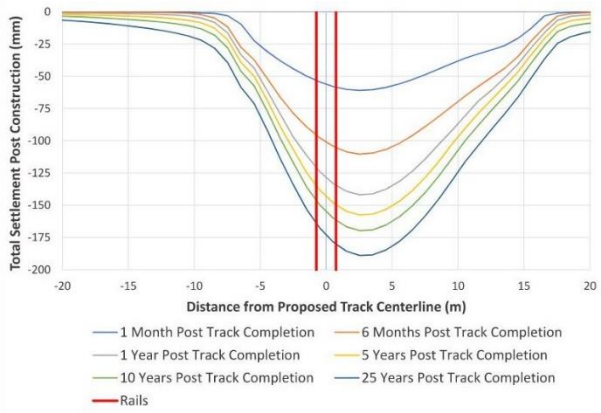

Figure 2. Anticipated Maximum Post-construction Differential Settlement Between Rails

5.4 Lateral Deformation

Though not modelled in Settle3, the results of the field trial program indicated that approximately 250 mm to 300 mm of lateral deformation in the downslope direction (west) could be expected to occur during construction. Furthermore, post-construction lateral creep of the embankment in the downslope direction was estimated to be approximately 50 mm to 60 mm over 25 years based on extrapolation of the results of the field trial program.

6 CONSTRUCTION SUMMARY

6.1 Embankment Construction Installation

A total of 2,988 Douglas fir round timber piles, approximately 15.2 m (50 ft) long with butt and tip diameters of approximately 360 mm (14 in) and 200 mm (8 in), respectively, were installed in a grid pattern with approximately 1.0 m ± 0.1 m centre-to-centre spacing. An excavator with a grapple attachment was used to partially install each pile as deep as practical, which generally corresponded to a depth of approximately 4.5 m to 6 m. The remaining length of each pile was driven by a drop-hammer with approximately 2 m to 3 m drop height, suspended from an 80-ton crawler crane within a period of about 6 minutes on average.

One layer of geocomposite biaxial geogrid and two layers of uniaxial geogrid were installed after the timber piles were driven to final depth. Accounting for settlement during construction, over 11,500 m^3 of fill material was placed to construct the embankment. Timber pile installation and embankment fill placement were completed as quickly as possible – within 70 days of the contractor mobilizing to site.

6.2 Instrumentation Monitoring During Construction

An observational approach was implemented to monitor both the landslide and performance of the embankment during construction due to the complex nature of the site. Multiple slope inclinometers, real-time tilt monitors and vibrating wire piezometers were installed to monitor

changes in ground conditions during construction and confirm that these changes were within acceptable limits.

6.2.1.1 Slope Inclinometers

Several slope inclinometers were installed both upslope and downslope of the embankment to monitor lateral deformation and assess whether the existing slip surface was being reactivated or any new slip surfaces were developing due to construction activity. Slope inclinometers were monitored daily during pile installation and embankment fill placement. Movement observed was generally concentrated in the upper 3 m to 5 m below ground level and correlated with lateral deformation as a result of pile installation and embankment fill material placement. Movement observed in the slope inclinometers generally ceased or significantly reduced after completion of pile installation and fill placement. Two slope inclinometers that were installed in close proximity to the toes of the embankment sheared due to the lateral deformation that occurred during construction. No evidence of deep-seated failure or reactivation of the slide was observed during construction.

6.2.1.2 Vibrating Wire Piezometers

Vibrating wire piezometers were installed within the embankment fill to monitor pore water pressures within the Glaciomarine Clay. The vibrating wire piezometers were installed between 3.5 m and 5.9 m below pre-construction ground level to be within the zone of influence of the embankment fill pressure. The piezometers were connected to dataloggers that collected and stored readings at short intervals of time. The data was reviewed at the end of each shift during construction to assess whether observed increases in pore water pressure were within acceptable limits.

Excess pore water pressures generated in the Glaciomarine Clay as a result of the placement of each lift of embankment fill generally dissipated within 24 hours to 48 hours. Due to the significant surface area of the embankment and the contractor's fill placement rate, placement of each lift of fill material generally began after the dissipation of the majority of the excess pore water pressure that was generated by the placement of the previous lift. As embankment height increased, the effect that fill placement had on pore water pressure generation diminished.

7 DISCUSSION AND CONCLUSIONS

The geotechnical investigation, analysis of material testing results, and construction field trial program provided key information that guided the design of the embankment, including estimates of key parameters required for the settlement analysis, as well as insight into the magnitudes of lateral displacement and excess pore water pressures that could be expected during construction. Results of the slope stability analyses that were completed were used to further refine the design, including the optimal angles of embankment slopes and reinforcement requirements to achieve the required live load FS.

The project was completed as quickly as possible to restore critical service to the track. Instrumentation monitoring carried out during construction was used to assess the response of the subgrade to loading and inform fill placement rates. Instrumentation monitoring is ongoing to assess the long-term performance of the embankment.

8 REFERENCES

Blais-Stevens, A., M. Geertsema and A. Grenier. 2017. Landslides in glaciomarine sediments in and around Lakelse Lake, Northwestern British Columbia.

Canadian Geotechnical Society (CGS). 2006. *Canadian Foundation Engineering Manual*, 4th ed.

Federal Highway Administration (FHWA). 2012. *Geosynthetic Reinforced Soil Integrated Bridge System, Interim Implementation Guide*. Publication No. FHWA HRT 11 026. U.S. Department of Transportation.

Forest Products Laboratory (FPL). 2010. *Wood Handbook – Wood as an Engineering Material*. General Technical Report FPL GTR 190. United States Department of Agriculture, Forest Service. Madison, WI.

Geertsema, M. and D.M. Cruden. 2014. Further travels in the Canadian Cordillera. *Proceedings, 6th Canadian conference on geohazards*. Kingston, ON.

Geertsema, M. and D.M. Cruden. 2008. Travels in the Canadian Cordillera. *4th Canadian conference on geohazards*.

Geertsema, M. and J. Schwab. 1996. A photographic Overview and Record of the Mink Creek Earth Flow, Terrace, British Columbia.

GEO-SLOPE International Ltd. (GEO-SLOPE). 2020. GeoStudio SLOPE/W Version 10.2.1.19666 [computer software].

Gere, J.M. and B.J. Goodno. 2009. *Mechanics of Materials*, 7th ed, Toronto: Cengage Learning.

Pile Dynamics, Inc. (Pile Dynamics). 2010. GRLWEAP [computer software].

Rocscience Inc. (Rocscience) 2011. RS2 Version 9.030 [computer software].

Rocscience Inc. (Rocscience) 2020. Settle3 Version 5.008 [computer software].

Southern Pressure Treaters' Association (SPTA). 2016. *Timber Pile Design and Construction Manual*.